Supplemental figure legends

Supplementary Figure 1. (A, B) Heat map showing the metabolites significantly affected in both yw and OreR females between 1 and 7 weeks of age.

Supplementary Figure 2. Venn diagrams for commonly changed metabolites between OreR and yw males (A), OreR and yw females (B), OreR females and males (C), yw females and males (D), OreR and yw males and females (E). (F) Principal component analysis of 1, 4 and 7 week yw and OreR males.

Supplementary Figure 3. (A) Relative mRNA levels of *dAhcyL1* from wandering third instar larval stage expressing *white (w)* RNAi (control), *dAhcyL1* RNAi-1 and *dAhcyL1* RNAi-2 under constitutive Actin5c-Gal4 driver. Means ± SD. (B) Relative mRNA levels of *dAhcyL2* from wandering third instar larval stage expressing *w* RNAi, *dAhcyL2* RNAi-1 or *dAhcyL2* RNAi-2 under constitutive Actin5c-Gal4 driver. Means ± SD. (C) Relative mRNA levels of *Ahcy13, dAhcyL1* and *dAhcyL2* in 1 week old control (B3) and long-lived (O1, O3) males. Means ± SD. (D) Relative mRNA levels of *Itp-r83A* from wandering third instar larval stage expressing *Itp-r83A* RNAi under constitutive Actin5c-Gal4 driver. **p<0.01. Means ± SD. (E) Relative mRNA levels of *RnrL* from wandering third instar larval stage expressing *RnrL* RNAi under constitutive Actin5c-Gal4 driver. **p<0.01. Means ± SD. (F) Relative mRNA levels of *Ahcy13* from wandering third instar larval stage expressing *w* RNAi (control) or *Ahcy13* RNAi-1 under the constitutive Actin5c-Gal4 driver. *p < 0.05. Means ± SD.

Supplementary Figure 4. Ubiquitous adult-onset expression of *dAhcyL1* RNAi does not affect lifespan in males under oxidative stress.

Supplementary Figure 5. Coimmunoprecipitation of overexpressed HA- and FLAG-tagged dAHCYL1 and Ahcy13 in *Drosophila* S2R cells. To test whether dAHCYL1 and Ahcy13 can form a heteromultimeric complex, we overexpressed HA- and FLAG-tagged dAHCYL1 and Ahcy13 in

Drosophila S2R cells. As expected FLAG-tagged dAHCYL1 and Ahcy13 were coimmunoprecipitated with their HA-tagged forms confirming that they form a homomultimeric complexes. Moreover, FLAG-tagged dAHCYL1 was coimmunoprecipitated with HA- tagged Ahcy13 suggesting that they form a heteromultimeric complexes as well.

Supplemental List 1. 21 common metabolites in "OreR Females 1-7w", "OreR Males 1-7w", "yw Females 1-7w" and "yw Males 1-7w":

1-Methyl-Histidine, betaine, Methionine sulfoxide, Carbamoyl phosphate, 2-Aminooctanoic acid, methionine, Cystathionine, allantoin, valine, UDP-N-acetyl-glucosamine, glutathione, UDP-D-glucose, glutathione-nega, Spermidine, cytidine, O8P-O1P, D-sedoheptulose-1-7-phosphate, tryptophan, L-arginino-succinate, SBP, acetoacetate

Supplemental_Methods

qRT-PCR. Total RNA was extracted with the TRIzol reagent (Life Technologies), followed by DNase digestion using RQ1 RNase-Free DNase (Promega). Total RNA was reverse transcribed with the iScript cDNA synthesis kit (Bio-Rad). qRT-PCR was performed with the iQ SYBR Green Supermix (Bio-Rad) and a CFX96 Real- Time PCR Detection System (Bio-Rad). *RpL32* and *alpha-Tubulin 84B* were used as a normalization reference. Relative quantitations of mRNA levels were determined with the comparative C_T method.

Antibodies and Immunoblot Analyses. Total histone antibody and H3K4Me3 antibody were obtained from Abcam, and the tubulin antibody from Sigma-Aldrich. For immunoblot analyses, 10 flies were grinded in bead beader in RIPA (Cell Signaling) lysis buffer. Whole-cell lysates were resolved by electrophoresis, and proteins were transferred onto PVDF membranes

(Immobilon P; Millipore), blocked in Tris-buffered saline Tween-20 buffer (Cell Signaling Technology) containing 2.5% dry milk, and probed with the indicated antibodies in this buffer.

Climbing Assays. Negative geotaxis assays were performed as previously described (Rhodenizer et al., 2008). Flies were gently tapped to the bottom of an empty plastic vial, and the number of flies that climbed to the top of the vial after 10s was scored.

Oxidative stress. For measuring resistance to oxidative stress induced by methyl viologen (Sigma), 40d old males were exposed to 10 mM methyl viologen in 5% sucrose solution. Dead flies were scored periodically.

Targeted Mass Spectrometry and data analyses. 20 flies per sample (5 biological replicates) were collected and intracellular metabolites were extracted using 1,6 mL of cold (-80°C) 80% (v/v) aqueous methanol. Flies were homogenized using 0.5 mm zirconium beads and insoluble material in lysates was centrifuged at 5,000*g* for 5 min, and the resulting supernatant was evaporated using a speed vac. Samples were re-suspended using 20 μL HPLC grade water for mass spectrometry. 10 μL were injected and analyzed using a 5500 QTRAP triple quadrupole mass spectrometer (AB/SCIEX) coupled to a Prominence UFLC HPLC system (Shimadzu) via selected reaction monitoring (SRM) of a total of 254 endogenous water soluble metabolites for steady-state analyses of samples. Some metabolites were targeted in both positive and negative ion mode for a total of 287 SRM transitions using positive/negative polarity switching. ESI voltage was +4900V in positive ion mode and –4500V in negative ion mode. The dwell time was 3 ms per SRM transition and the total cycle time was 1.55 seconds. Approximately 10-14 data points were acquired per detected metabolite. Samples were delivered to the mass spectrometer via normal phase chromatography using a 4.6 mm i.d x 10 cm Amide Xbridge HILIC column (Waters Corp.) at 350 μL/min. Gradients were run starting from 85% buffer B (HPLC grade acetonitrile) to 42% B from 0-5 minutes; 42% B to 0% B from 5-16 minutes; 0% B

was held from 16-24 minutes; 0% B to 85% B from 24-25 minutes; 85% B was held for 7 minutes to re-equilibrate the column. Buffer A was comprised of 20 mM ammonium hydroxide/20 mM ammonium acetate (pH=9.0) in 95:5 water:acetonitrile. Peak areas from the total ion current for each metabolite SRM transition were integrated using MultiQuant v2.0 software (AB/SCIEX).

The resulting raw data from the MultiQuant software were uploaded in metaboanalyst (http://www.metaboanalyst.ca/MetaboAnalyst/) and subsequent data processing and analyses were performed using this tool. Metabolites that were not detected in 40% of the samples were excluded from the analysis. Data were normalized to the median (per sample) and processed through log transformation. Heat map and hierarchical clustering was generated using Pearson correlations and Ward's method. Metabolite Set Enrichment Analysis (MSEA) was performed using Metaboanalyst which uses the KEGG (http://www.genome.jp/kegg/pathway.html) pathway database. Metabolite sets containing at least 5 compounds were employed in the analysis. MSEA calculates hypergeometrics test scores based on cumulative binominal distribution.

Primers for qRT-PCR

Primers for qRT-PCR were designed in accordance to (Hu et al., 2013).

Gene	**FlyPrimerBank ID**	**Forward Primer**	**Reverse Primer**
CG9977 (dAhcyL1)	PP26084	GGCGAGACGGAAGAGGACT	AGAGAGCTGATAGAGAC GGTG
Ahcy89E (*dAhcyL2*)	PP37398	AAGAGTGCATTTGGAAGGCG	ACCCTTTAGGGGCTTCT CATC
Ahcy13	PP36991	AGCCCCTGAACATGATCCTG	CGACCCTCCTTGAACAT

			CTTGT
Itp-r83A	PP16906	CGGTTTCTTGAGCACACTCG	CTGAACTTCTTAGGCGGACAG
RnrL	PP11723	CCTGTTACTATCACCCTGCAAG	AGGATGGCGTAGTCGGGAT
LacZ		GAGAATCCGACGGGTTGTTA	GACAGTATCGGCCTCAGGAA

Supplemental Table 1. List of lines tested for the effect on lifespan:

#	CG#	RNAi or ORF line ID
1	CG10160	HMS00039
2	CG10621	HMS02412
	CG10621	FL4205
3	CG10623	HMC02683
4	CG10692	HMS10667
5	CG10692	HMS02599
	CG10692	HMC03318
6	CG10903	10903R-1 (II)
7	CG11134	JF03052
	CG11334	v109672
	CG11334	FL0052
8	CG11654	HMC03222
9	CG12173	HMJ21083

10	CG13598	HMC03239
11	CG1461	HMC03212
12	CG14882	HMC04302
13	CG15100	ORF-3xHA F000999
	CG15100	HMC04303
14	CG17230	17230R-2
	CG17230	HMC04543
15	CG1753	HMS03028
16	CG2674	JF03351
17	CG2759	HMS00017
18	CG31322	HMC04301
19	CG32068	v106831
	CG32068	HMC04304
20	CG4067	HMS02643
21	CG4210	HMC02982
22	CG4300	v105402
	CG4300	FL2564 CG4300
	CG4300	HMC03665
23	CG4743	HMC04321
24	CG4802	4802R-2 (II)
	CG4802	FL3987 CG4802
25	CG5029	v101753/KK

26	CG5345	HMS03027
27	CG5493	v50637
28	CG6188	HMC03498
	CG6188	FL2157 CG6188
	CG6188	HMS02473
29	CG6584	HMC03659
30	CG7266	HMS02570
31	CG7560	7560R-1 (II)
32	CG8290	JF02410
33	CG8327	8327R-2 (III)
	CG8327	FL1085 CG8327
34	CG8956	8956R-1
	CG8956	HMJ23469
35	CG9977	HM05009
	CG9977	G4143
	CG9977	HMC04803

Supplemental_Fig_S1

A

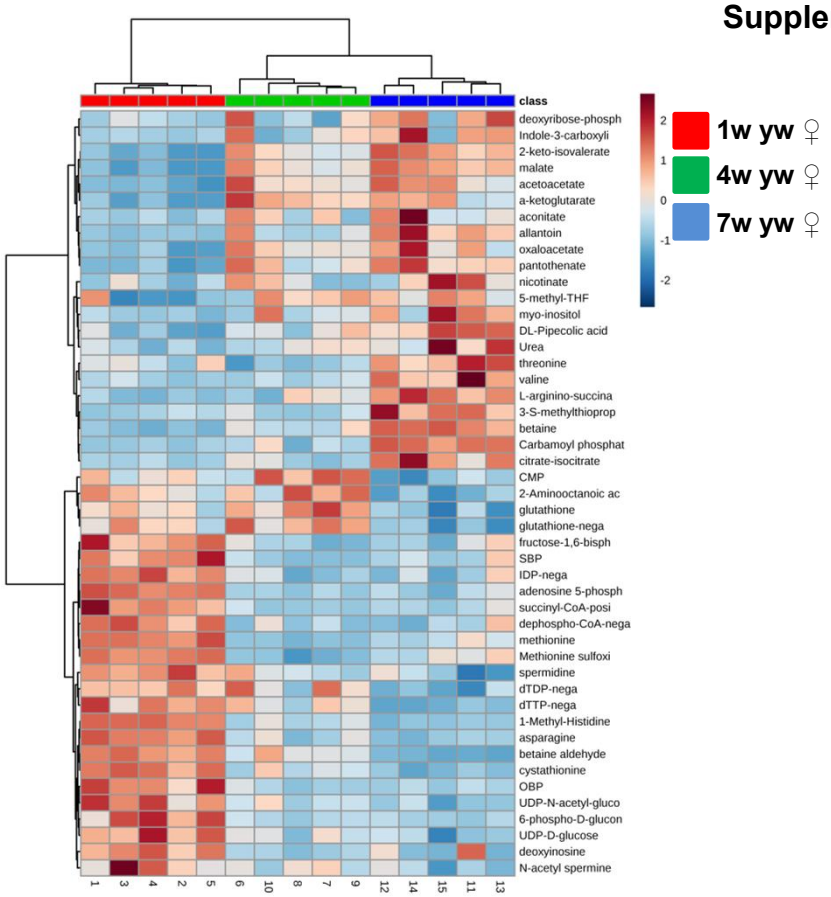

B

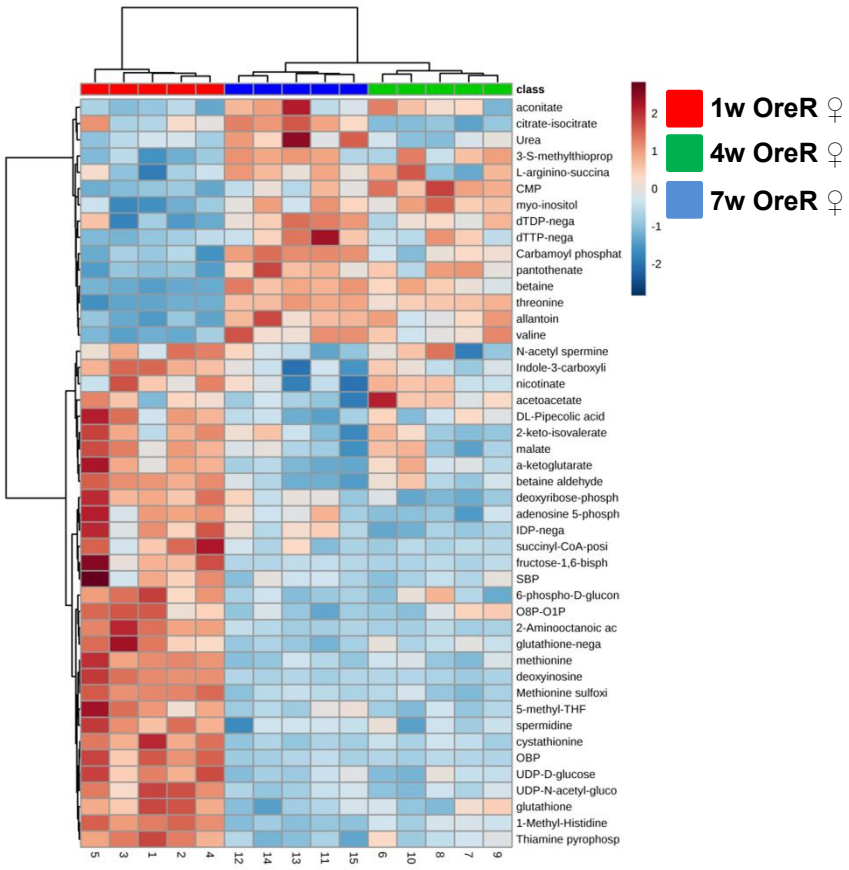

A

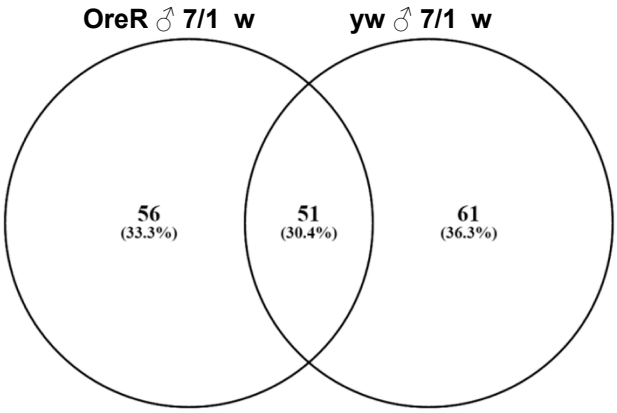
OreR ♂ 7/1 w
yw ♂ 7/1 w
56 (33.3%)
51 (30.4%)
61 (36.3%)

B

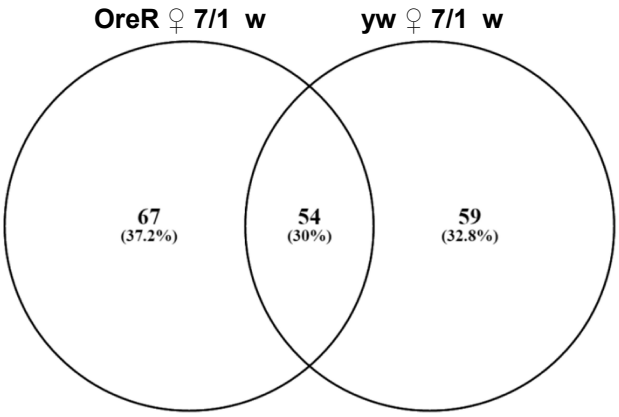
OreR ♀ 7/1 w
yw ♀ 7/1 w
67 (37.2%)
54 (30%)
59 (32.8%)

C

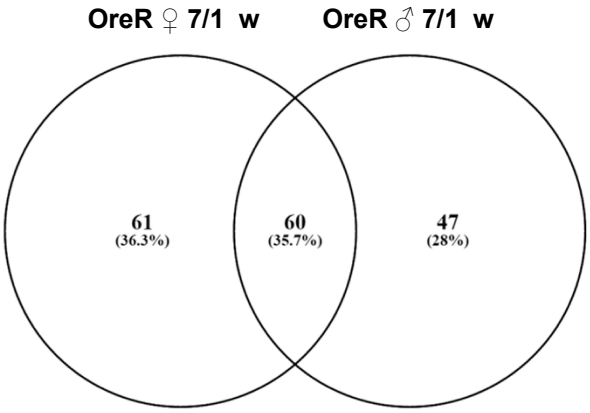
OreR ♀ 7/1 w
OreR ♂ 7/1 w
61 (36.3%)
60 (35.7%)
47 (28%)

D

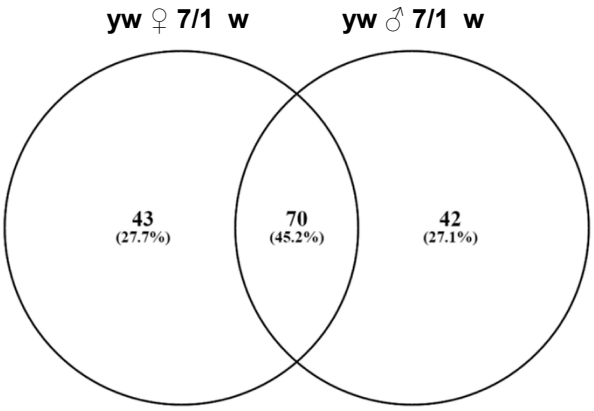
yw ♀ 7/1 w
yw ♂ 7/1 w
43 (27.7%)
70 (45.2%)
42 (27.1%)

E

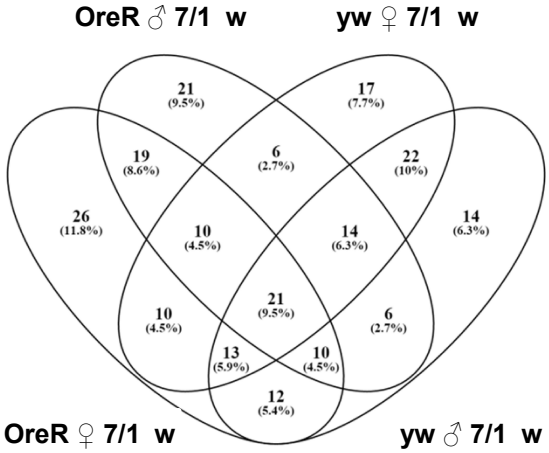
OreR ♂ 7/1 w
yw ♀ 7/1 w
21 (9.5%)
17 (7.7%)
19 (8.6%)
6 (2.7%)
22 (10%)
26 (11.8%)
10 (4.5%)
14 (6.3%)
14 (6.3%)
10 (4.5%)
21 (9.5%)
6 (2.7%)
13 (5.9%)
10 (4.5%)
12 (5.4%)
OreR ♀ 7/1 w
yw ♂ 7/1 w

F

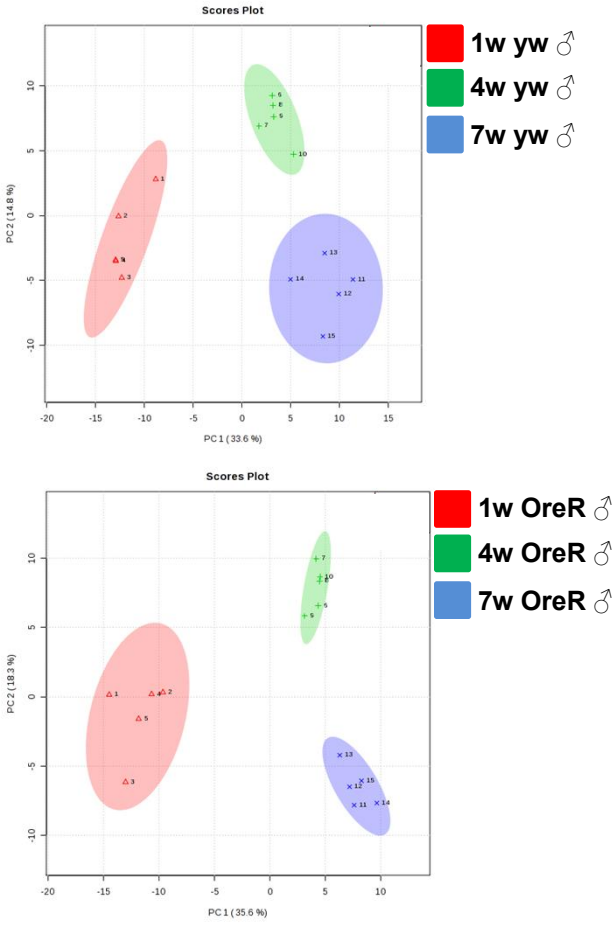
Scores Plot
1w yw ♂
4w yw ♂
7w yw ♂
PC 1 (33.6 %)
PC 2 (14.8 %)
Scores Plot
1w OreR ♂
4w OreR ♂
7w OreR ♂
PC 1 (35.6 %)
PC 2 (18.3 %)

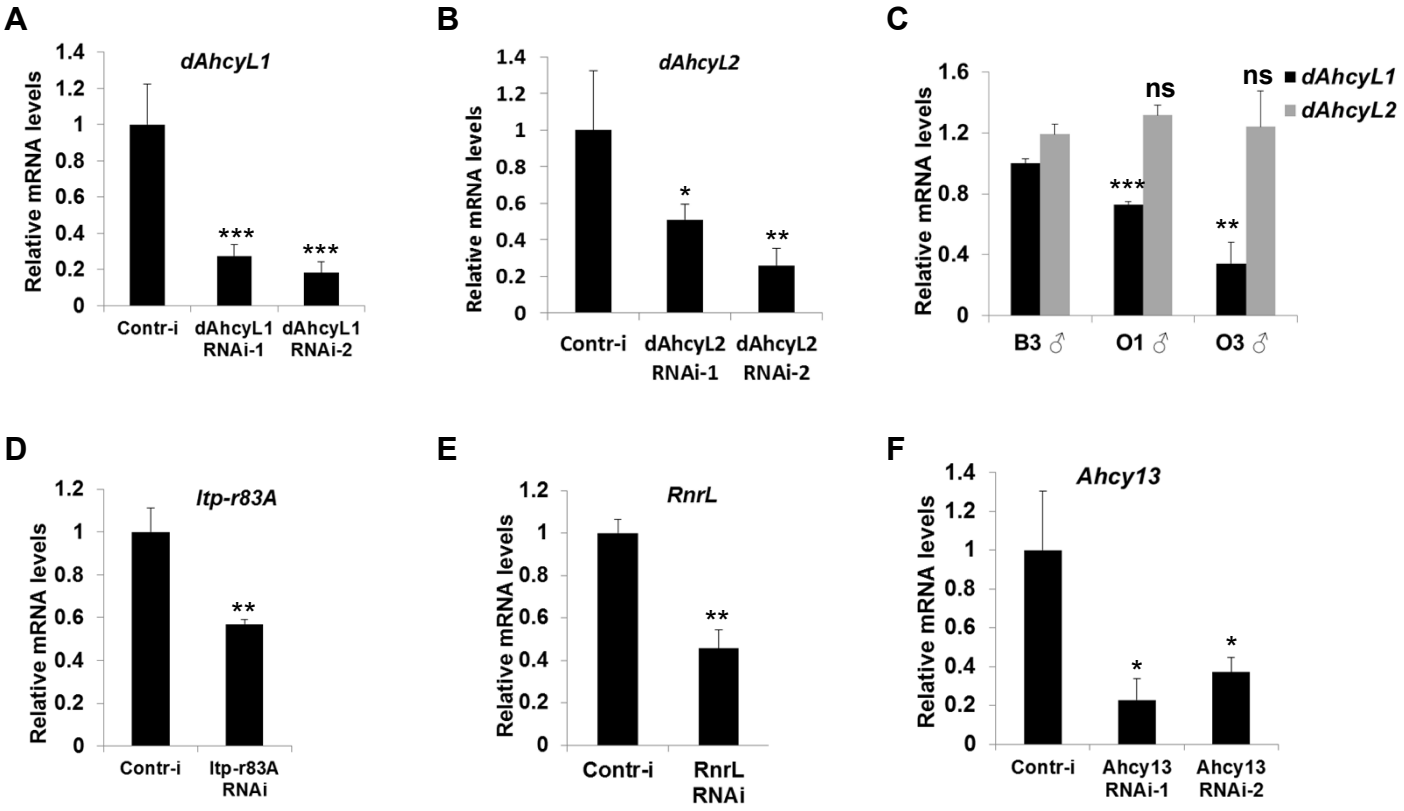
A
dAhcyL1
Relative mRNA levels
1.4
1.2
1
0.8
0.6
0.4
0.2
0
***
***
Contr-i
dAhcyL1 RNAi-1
dAhcyL1 RNAi-2
B
dAhcyL2
Relative mRNA levels
*
**
Contr-i
dAhcyL2 RNAi-1
dAhcyL2 RNAi-2
C
Relative mRNA levels
1.6
1.2
0.8
0.4
0
ns
ns
***
**
dAhcyL1
dAhcyL2
B3 ♂
O1 ♂
O3 ♂
D
Itp-r83A
Relative mRNA levels
**
Contr-i
Itp-r83A RNAi
E
RnrL
Relative mRNA levels
**
Contr-i
RnrL RNAi
F
Ahcy13
Relative mRNA levels
*
*
Contr-i
Ahcy13 RNAi-1
Ahcy13 RNAi-2

Supplemental_Fig_S4

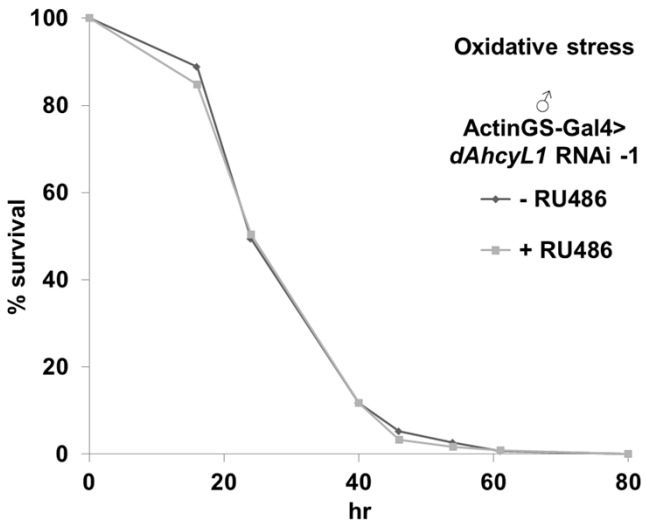

Supplemental_Fig_S5